

Complementarity between dark matter direct searches and CE ν NS experiments in $U(1)'$ models

Leon M. G. de la Vega,^{1,*} L. J. Flores,^{1,†} Newton Nath,^{1,‡} and Eduardo Peinado^{1,§}

¹*Instituto de Física, Universidad Nacional Autónoma de
México, A.P. 20-364, Ciudad de México 01000, México.*

We explore the possibility of having a fermionic dark matter candidate within $U(1)'$ models for CE ν NS experiments in light of the latest COHERENT data and the current and future dark matter direct detection experiments. A vector-like fermionic dark matter has been introduced which is charged under $U(1)'$ symmetry, naturally stable after spontaneous symmetry breaking. We perform a complementary investigation using CE ν NS experiments and dark matter direct detection searches to explore dark matter as well as Z' boson parameter space. Depending on numerous other constraints arising from the beam dump, LHCb, BABAR, and the forthcoming reactor experiment proposed by the SBC collaboration, we explore the allowed region of Z' portal dark matter.

I. INTRODUCTION

The coherent-elastic neutrino-nucleus scattering (CE ν NS) has been observed by the COHERENT collaboration using cesium-iodide (CsI) detector [1], almost 40 years after of its first proposal [2]. The reported results are observed at 6.7σ significance and are consistent with the Standard Model (SM) expectations at 1.5σ [1]. Recently, the first measurement of CE ν NS using the CENNS-10 liquid argon detector [3, 4] has been reported by the COHERENT collaboration with greater than 3σ significance. For this process to occur, neutrino energies below ~ 50 MeV are needed, hence producing nuclear recoil energies of a few keV. Detecting nuclear recoils with such low energy is the major challenging task for any experiment.

Therefore, the measurement of such low-energy process opens a new window to study and test the SM at low momentum transfer [5–8], nuclear physics [9–12], as well as neutrino electromagnetic properties [8, 13].

In recent times, many studies suggest that CE ν NS is an excellent complement to test new physics beyond the SM, like sterile neutrinos [14–17], or even non-standard neutrino interactions [18–23].

* leonm@estudiantes.fisica.unam.mx

† luisjf89@fisica.unam.mx

‡ newton@fisica.unam.mx

§ epeinado@fisica.unam.mx

However, here we are interested to investigate dark matter (DM) using these neutrino-nucleus scattering experiments. It has been known in literature that there exists numerous amount of astrophysical and cosmological evidence for the existence of DM in the universe, but so far there is no experimental result, neither from direct/indirect detection nor from accelerator-based experiments, that supports its existence.

Among the many dark matter candidates, the thermally produced Weakly Interacting Massive Particle (WIMP) has received much theoretical and experimental scrutiny. Many dark matter direct detection experiments, such as the Xenon1T [25] or PandaX-II [26] experiments for example, have also set stringent limits on the DM - nucleus cross-section. In particular, there exists some interesting light mediators models connecting dark photons with the light dark matter, as pointed in [27–33]. Moreover, the COHERENT collaboration has recently studied sub-GeV dark matter models using detector sensitive to CE ν NS processes in Ref. [34].

In this work, we exploit an extension of the SM consisting of an additional anomaly-free $U(1)'$ gauge symmetry with a very light gauge boson, Z' , and a dark matter candidate, stable due to a residual symmetry of $U(1)'$. There exists very well-motivated studies, where a new $U(1)'$ gauge symmetry arises, namely, in the context of supersymmetry [35–37], grand unified theories [38–40], and string-motivated models [41, 42]. We will study different scenarios for the $U(1)'$ where dark matter is charged under this symmetry, quarks have flavor independent charges, while leptons are allowed to have generation-dependent charge, namely $U(1)_{B-L}$, $U(1)_{B-2L_\alpha-L_\beta}$, and $U(1)_{B-3L_\alpha}$. In this way the new gauge boson couples to quarks, leptons, and dark matter. If the interaction mediates both processes, namely dark matter - nucleus scattering and an extra contribution to neutrino - nucleus scattering, there will be a correlation between both cross-sections. In particular, if an extended gauge symmetry is considered to mediate both processes, the couplings are also correlated through the gauge coupling and the vector boson mediator mass. The light gauge boson will mediate the interaction between dark matter and nuclei and it will also contribute to the interaction of a neutrino with nuclei. We will focus on the complementarity of the searches for light gauge bosons and dark matter from colliders and CE ν NS experiments.

Furthermore, considering the combined effect of different experimental constraints coming from the COHERENT collaboration, beam-dump experiments, the LHCb and the BABAR dark photon searches, we examine the allowed parameter space to constrain Z' boson and dark matter for each $U(1)'$ models. In addition, we also explore the potential of upcoming reactor-based CE ν NS experiment proposed by the Scintillating Bubble Chamber (SBC) collaboration [43, 44]. Bounds arising from astrophysical observations such as Big Bang Nucleosynthesis (BBN) and Cosmic Microwave

Background (CMB) have also been shown for the comparison.

We organize this work as follows. Sec. II is dedicated to a brief description of CE ν NS experiments. Dark matter in $U(1)'$ models has been discussed in Sec. III. We discuss the DM relic density and direct detection process in Sec. IV. Our principal results are illustrated in Sec. V. Summary of this work and concluding remarks are presented in Sec. VI.

II. CE ν NS PROCESSES AND Z' BOSON

The coherent elastic neutrino-nucleus scattering (CE ν NS) was measured by the COHERENT experiment [1] using neutrinos from a stopped-pion source at the Spallation Neutron Source (SNS) at Oak Ridge National Laboratory. The COHERENT collaboration used two different detectors, one made of CsI [1] and the other one made of LAr [45].

Furthermore, there are several experiments trying to measure CE ν NS using reactor antineutrinos, but the need of sub-keV thresholds and great control over background has made this task difficult. One of these experimental proposals is a liquid argon scintillating bubble chamber, currently under construction by the SBC collaboration [43, 44]. With an expected energy threshold of 100 eV, a 10-kg chamber placed near a 1-MW_{th} nuclear reactor will be able to measure SM parameters with high precision, such as the weak mixing angle, in addition to set competitive limits on some beyond SM scenarios [44].

The SM differential cross-section for CE ν NS process is given by [46–48]

$$\frac{d\sigma}{dT} = \frac{G_F^2}{2\pi} M_N Q_w^2 \left(2 - \frac{M_N T}{E_\nu^2} \right), \quad (1)$$

where T is the nuclear recoil energy, E_ν is the incoming neutrino energy, and M_N is the nuclear mass. The weak nuclear charge, Q_w , is given by ¹

$$Q_w = Z g_p^V F_Z(Q^2) + N g_n^V F_N(Q^2), \quad (2)$$

where $g_p^V = 1/2 - 2\sin^2\theta_W$ and $g_n^V = -1/2$ are the SM weak couplings, Q is the transferred momentum, $Z(N)$ is the proton (neutron) number of the nucleus, and $F_{Z(N)}(Q^2)$ the nuclear form factor. Since $g_p^V \sim 0.02$, the cross-section depends highly on the number of neutrons N .

In presence of a new vector interaction, the cross-section for CE ν NS is affected through the weak nuclear charge (see Eq. (2)) in the following way:

$$Q_{w\alpha} = Z(g_p^V + 2\varepsilon_{\alpha\alpha}^{uV} + \varepsilon_{\alpha\alpha}^{dV})F_Z(Q^2) + N(g_n^V + \varepsilon_{\alpha\alpha}^{uV} + 2\varepsilon_{\alpha\alpha}^{dV})F_N(Q^2), \quad (3)$$

¹ Neglecting the axial-vector interaction.

where $\varepsilon_{\alpha\alpha}^{u(d)V}$ are the parameters that quantify the strength of the new interaction (relative to the weak scale) with $u(d)$ quarks, and $\alpha = (e, \mu, \tau)$. Notice that with this new contribution, the differential cross-section from Eq. (1) is now flavor dependent. The effective low-energy Lagrangian for the neutrino-quark interactions with a new Z' boson can be written as

$$\mathcal{L}_{\text{eff}} = -\frac{g'^2}{Q^2 + M_{Z'}^2} \left[\sum_{\alpha} x_{\alpha} \bar{\nu}_{\alpha} \gamma^{\mu} P_L \nu_{\alpha} \right] \left[\sum_q x_q \bar{q} \gamma_{\mu} q \right], \quad (4)$$

where g' and $M_{Z'}$ are the coupling and mass of the new gauge boson, respectively. Therefore, by comparing this effective Lagrangian with the one from an effective field theory approach, we can relate the $\varepsilon_{\alpha\alpha}^{u(d)V}$ parameters with the Z' interaction parameters as

$$\varepsilon_{\alpha\alpha}^{u(d)V} = \frac{g'^2 x_{\alpha} x_q}{\sqrt{2} G_F (Q^2 + M_{Z'}^2)}. \quad (5)$$

In order to extract limits on the Z' parameters from the measurement by the COHERENT collaboration with the CsI detector, the following χ^2 function can be used [1]

$$\chi^2 = \sum_{i=4}^{15} \left[\frac{N_{\text{meas}}^i - (1 + \alpha) N_{\text{th}}^i - (1 + \beta) B_{\text{on}}^i}{\sigma_{\text{stat}}^i} \right]^2 + \left(\frac{\alpha}{\sigma_{\alpha}} \right)^2 + \left(\frac{\beta}{\sigma_{\beta}} \right)^2, \quad (6)$$

where N_{meas}^i and N_{th}^i are the measured and theoretical predicted number of events per energy bin, respectively, $\sigma_{\text{stat}}^i = \sqrt{N_{\text{meas}}^i + B_{\text{on}}^i + 2B_{\text{ss}}^i}$ is the statistical uncertainty of the measurement, and $B_{\text{on}}^i (B_{\text{ss}}^i)$ is the beam-on (steady-state) background. The systematic uncertainties of signal and background normalization are encoded in $\sigma_{\alpha} = 0.28$ and $\sigma_{\beta} = 0.25$, respectively. The function in Eq. (6) has to be marginalized over α and β , which are nuisance parameters. Recently it has been shown that the limits for a light vector mediator obtained from the COHERENT measurements with the LAr detector are similar to the ones obtained with the CsI data [23, 49, 50]. Therefore, in this work we will present bounds only from the CsI measurement.

For the case where there is no current measurement, such as with the SBC-CE ν NS detector, one can assume the measured signal as the SM expectation plus background. Hence, the projected sensitivities on the Z' parameters can be obtained with the χ^2 function

$$\chi^2 = \left[\frac{N_{\text{meas}} - (1 + \alpha) N_{\text{th}}(\gamma) - (1 + \beta) B_{\text{reac}}}{\sigma_{\text{stat}}} \right]^2 + \left(\frac{\alpha}{\sigma_{\alpha}} \right)^2 + \left(\frac{\beta}{\sigma_{\beta}} \right)^2 + \left(\frac{\gamma}{\sigma_{\gamma}} \right)^2, \quad (7)$$

where B_{reac} is the background due to the nuclear reactor. Here, the statistical uncertainty is defined as $\sigma_{\text{stat}} = \sqrt{N_{\text{meas}} + 4B_{\text{cosm}}}$, with B_{cosm} the background from muon-induced and cosmogenic neutrons. The nuclear recoil threshold is set to $(1 + \gamma) \cdot 100$ eV, where γ is an additional nuisance parameter, while the systematic uncertainties associated to the signal, background, and energy threshold are set to $\sigma_{\alpha} = 0.024$, $\sigma_{\beta} = 0.1$, and $\sigma_{\gamma} = 0.05$, respectively.

Symmetry/Field	Q	u	d	L_e	L_μ	L_τ	e_e	e_μ	e_τ	N_1	N_2	N_3	H
$U(1)'$	1/3	1/3	1/3	x_e	x_μ	x_τ	x_e	x_μ	x_τ	x_e	x_μ	x_τ	0

TABLE I. $U(1)'$ charges of the model. The charges x_α , with $\alpha = e, \mu, \tau$, can take the values $x_\alpha = 0, -1, -2, -3$, while the charges of the quarks are 1/3.

III. DARK MATTER IN A $U(1)'$ EXTENSION OF THE STANDARD MODEL

The $U(1)'$ extension of the SM consists of an extra local gauge symmetry. In our framework the SM fermions are charged under the additional $U(1)'$, while the SM Higgs doublet is left uncharged, as shown in Table I. Scalar singlets ϕ_i are added in order to spontaneously break $U(1)'$ symmetry as given by Table II. Leptons are charged according to flavor-dependent charges x_e, x_μ and x_τ . Anomaly cancellation conditions restrict the possible set of lepton charges $\{x_e, x_\mu, x_\tau\}$. We consider the solution $\{-1, -1, -1\}$ corresponding to the well-known $B - L$ model, solutions $\{-1, -2, 0\}$, $\{-1, 0, -2\}$, $\{0, -1, -2\}$ and $\{0, -2, -1\}$ corresponding to $B - 2L_\alpha - L_\beta$ models with very specific predictions in the leptonic sector [23] as well as solutions $\{-2, -1, 0\}$, $\{-2, 0, -1\}$. Finally, solutions $\{-3, 0, 0\}$, $\{0, -3, 0\}$ and $\{0, 0, -3\}$ have been considered for the $B - 3L_\alpha$ model [53–55].

It is well known that if we extend the SM with a $U(1)'$ symmetry spontaneously broken by a scalar field with a integer charge, it is possible to have a residual symmetry Z_N . This happens if there is a scalar or fermion field with fractional $U(1)'$ charge [56]. This mechanism can be responsible for the DM stability and depending on the symmetry it can also tell us if neutrinos are Dirac or Majorana particles [57, 58]. Consider introducing a SM singlet fermion χ which can be Dirac or Majorana, depending only on its $U(1)'$ charge. To avoid spoiling the anomaly-free nature of the model a vector-like pair of χ , χ_L and χ_R , is needed. If $\chi_{L/R}$ transform as 1/2, they will be a pair of Majorana fields and their mass will be provided once the $U(1)'$ is broken by a flavon field ϕ transforming as 1 under $U(1)'$. On the other hand, if $\chi_{L/R}$ transform as 1/3 they will form a Dirac fermion. Thus, we end up with a residual Z_3 symmetry, which stabilizes the DM.

For the choice of Dirac fermion charge 1/3 the resulting dark matter mass eigenstate is given by $\chi = \chi_L + \chi_R$. We can write the dark sector Lagrangian as follows

$$\mathcal{L}_D = \left(\bar{\chi} \gamma^\mu (\partial_\mu + i \frac{g'}{3} Z'_\mu) \chi \right) + M_\chi \bar{\chi} \chi + h.c. \quad (8)$$

The only coupling of χ is therefore to the Z' gauge boson. The relic density of dark matter may be determined by this coupling in the *freeze-out* regime, through the Z' mediated $\bar{\chi} \chi \rightarrow \bar{f} f$ channel, where f is a SM fermion, as well as the $\bar{\chi} \chi \rightarrow Z' Z'$ channel. The Z' channel also provides a tree-level spin-independent direct detection signature. It is well known that these two constraints

	$U(1)'$ models	Scalar Fields	Masses of Z' ($M_{Z'}^2$)
MI	$U(1)_{B-L}$	ϕ_2	$g'^2(4v_2^2)$
MII	$U(1)_{B-2L_\alpha-L_\beta}$	ϕ_1, ϕ_2	$g'^2(v_1^2 + 4v_2^2)$
MIII	$U(1)'_{B-2L_\alpha-L_\beta}$	ϕ_1, ϕ_2, ϕ_4	$g'^2(v_1^2 + 4v_2^2 + 16v_4^2)$
MIV	$U(1)_{B-3L_\alpha}$	ϕ_3, ϕ_6	$g'^2(9v_3^2 + 36v_6^2)$

TABLE II. Singlet scalar fields ϕ_i having charges i under $U(1)'$.

(freeze-out relic density and direct detection bounds) are in tension for $m_\chi < \mathcal{O}(10 \text{ TeV})$ in $U(1)'$ models [60–66]. For DM masses below $\mathcal{O}(10) \text{ GeV}$ the direct detection bounds are much less stringent, due to poor detector sensitivity to nuclear recoils induced by the light dark matter. For the light dark matter and light Z' , the correct relic density is obtained for gauge couplings of order $0.1 - 1$, which are excluded by CE ν NS experiments. This motivates the use of an annihilation cross-section enhancement mechanism. To avoid enlarging the field content of the model, we consider the resonant Z' mechanism, where $M_\chi \sim M_{Z'}/2$. We parametrize the resonant condition with the δ_{Res} parameter defined by the relation

$$M_\chi = \frac{M_{Z'}}{2} (1 + \delta_{\text{Res}}). \quad (9)$$

We implemented the $U(1)'$ models in LanHEP [67] and micrOMEGAs [68] to calculate the dark matter observables, scanning over the ranges $(10^{-3} - 50) \text{ GeV}$ for the Z' mass, $(10^{-6} - 10^{-1})$ for the g' gauge coupling and to ensure the resonant annihilation $(0.45 - 0.55) M_{Z'}$ for M_χ , varying $|\delta_{\text{Res}}|$ between $(0.001 - 0.1)$.

For the different models we will need different singlet scalar fields ϕ_i transforming as i under the $U(1)'$, as shown in Table II, in order to obtain phenomenologically viable neutrino mass matrices through the type-I seesaw mechanism. The Z' boson, after $U(1)'$ breaking by the scalars, obtains the mass $M_{Z'}$ for different models as shown in Table II. The fields we have included are those who give a correct neutrino masses and mixings. For **MI** there are no correlations in the active neutrino mass matrix, for **MII** there are four cases with good phenomenology and predictions as investigated in [23], for **MIII** there is one correlation, see Appendix A and for **MIV** there are no correlations.

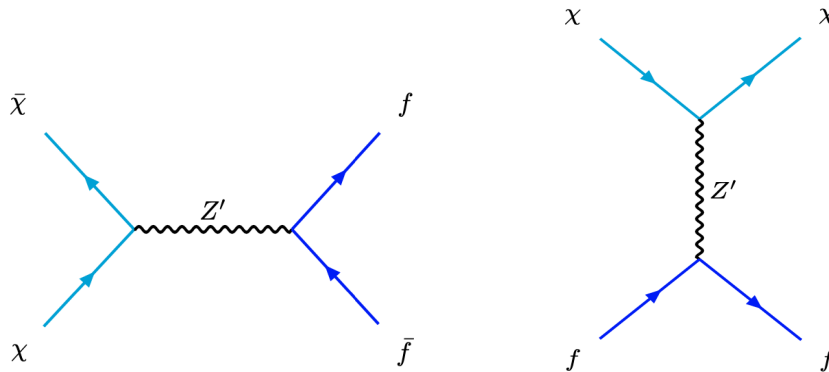


FIG. 1. Feynman diagrams leading to dark matter annihilation in the thermal *freeze-out* process (left) and dark matter direct detection (right).

IV. RELIC DENSITY AND DIRECT DETECTION

In this work we investigate the possibility of χ being a thermally produced WIMP dark matter candidate, taking into account experimental Z' constraints to its possible couplings to the SM fields. The relic density of χ is determined by the thermal *freeze-out* with resonant enhancement of the Z' mediated annihilation cross-section. The kinematically allowed processes are $\bar{\chi}\chi \rightarrow \bar{f}f$ for SM fermions f with masses $M_f > M_\chi$, as shown in Fig. 1 (see left panel). The t-channel $\bar{\chi}\chi \rightarrow Z'Z'$ process is kinematically forbidden by the resonance condition $2M_\chi \sim M_{Z'}$. In the parameter space considered here, the leading contributions to the relic density determination are the annihilation into neutrinos, followed by charged leptons, while quarks contribute $\mathcal{O}(1 - 10\%)$. The resonant condition allows lower values of g' compared to the non-resonant case down to $g' \sim 10^{-6}$ for a 50 MeV Z' mass, for example. We filter the data to reproduce the observed relic density $\Omega_{\text{CDM}}h^2 = 0.1198$ [69].

The gauge coupling of DM to the Z' leads to tree level spin-independent (SI) scattering of DM with nucleons. The Feynman diagram corresponding to this process is shown in Fig. 1 (see right panel). The most stringent limits on the elastic SI nucleon-DM scattering to date have been obtained by the Xenon1T [25] and PandaX-II [26] collaborations. The SI scattering limits weaken as the DM mass drops below ~ 20 GeV. Future experiments are projected to explore this low region mass, down to the neutrino floor. One such experiment is the SBC-DM [43] in its future dark matter 1 ton-yr phase. We consider both current Xenon1T and PandaX-II results as well as the 1 ton-yr SBC-DM projection.

The dark matter-nucleus SI cross-section per nucleon, in the small momentum transfer limit, is

given by [70]

$$\sigma_{\text{SI}} \approx \frac{\mu_{\chi n}^2}{\pi} \frac{(Zf_p + (A - Z)f_n)^2}{A^2}, \quad (10)$$

where, $\mu_{\chi n}$ is the WIMP-nucleon reduced mass, Z , A are the atomic number, atomic mass of the target nucleus, respectively. Also, f_p and f_n represent proton and neutron scattering functions and are given by

$$f_p \approx \frac{g_\chi}{M_{Z'}^2} (2g_u + g_d), \quad f_n \approx \frac{g_\chi}{M_{Z'}^2} (g_u + 2g_d). \quad (11)$$

In this study, $g_u = g_d = g_\chi = g'/3$, hence $f_p = f_n \approx \frac{g'^2}{3M_{Z'}^2}$. Therefore, the spin-independent cross-section reduces to

$$\sigma_{\text{SI}} \approx \frac{\mu_{\chi n}^2}{\pi} \frac{g'^4}{9M_{Z'}^4}. \quad (12)$$

Due to the vector-like nature of χ , axial couplings to Z' of the form $g_A \bar{\chi} \gamma^\mu \gamma_5 Z'_\mu \chi$ are not present at tree-level. Therefore, the spin dependent scattering cross-section arises at one-loop level and is consequently subdominant. Hence, we consider only constraints coming from SI scattering experiments. Given the resonance condition $2M_\chi \sim M_{Z'}$, we can project the constraints from direct detection experiments to the $M_{Z'} - g'$ parameter space utilizing Eq. (12). Conversely, we can project the constraints on $M_{Z'} - g'$ from CE ν NS, collider, beam dump, and cosmology to the $M_\chi - \sigma_{\text{SI}}$ parameter space.

V. DARK MATTER DIRECT DETECTION AND CE ν NS COMPLEMENTARITY

Here, we present our numerical results in search of Z' boson as well as DM considering various constraints arising from both the dark matter direct detection experiments as well as experiments searching for CE ν NS processes. Moreover, in order to have a comprehensive understanding of the allowed parameter space, constraints arising from various other experiments are also presented. In the left panel, exclusion regions are shown using different color in the $(M_{Z'} - g')$ plane, whereas in the right-panel we show exclusion limits for $(M_\chi - \sigma_{\text{SI}})$ plane. We start our discussion by analyzing the flavor-independent $U(1)'$ (i.e., $U(1)_{B-L}$) model, which is shown in Fig. (2). The constraints arising from the COHERENT-CsI data has been presented using the light-purple shaded region. The exclusion regions arising from the future reactor-based CE ν NS experiment SBC-CE ν NS [43, 44] are shown using the black long-dashed line. In order to present results for these CE ν NS experiments in the $(M_{Z'}, g')$ plane, we perform a χ^2 test using the latest COHERENT-CsI

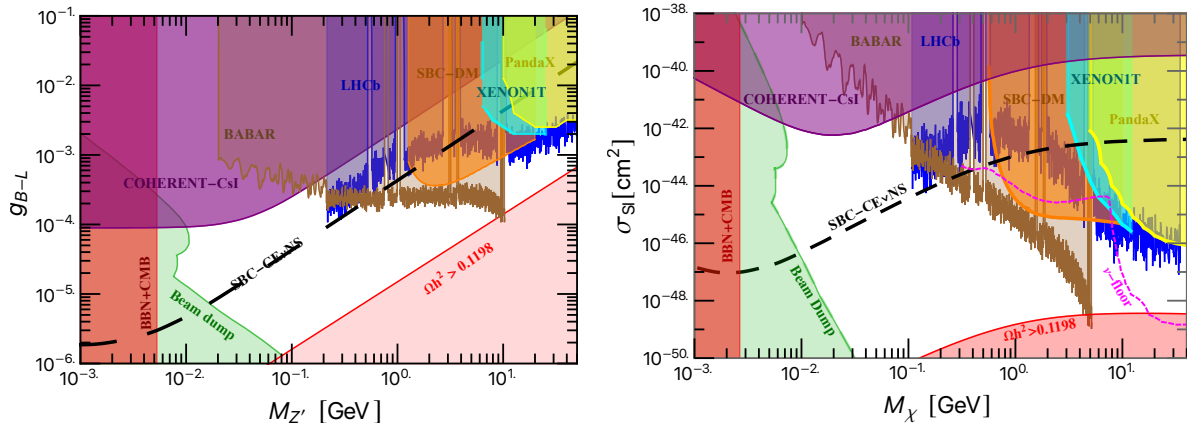


FIG. 2. Left panel: Exclusion regions in the $(M_{Z'}, g')$ plane for the B-L model. Right panel: Exclusion regions for the spin independent cross-section in the (M_{χ}, σ_{SI}) plane for the B-L model. The light-purple shaded area corresponds to the constraint set by the current COHERENT-CsI data [1]. The limits set by the future reactor-based CE ν NS experiment SBC [43, 44], is presented using the black long dashed line (SBC-CE ν NS). The exclusion regions set by the BBN and CMB [71], beam dump experiments [72–82], BABAR [83] and LHCb dark photon searches [84] are presented using the red, light-green, light-brown and sky-blue regions, respectively. Limits set by the dark matter experiments are presented using the light-orange, light-cyan, and light-yellow regions for the SBC-DM [43], XENON1T [25], and PandaX-II [26] experiments, respectively (see text for more details). In the right panel, the argon ν -floor background [85] has been marked using dotted-magenta curve.

data [1] as well as for the SBC-CE ν NS [43, 44], following numerical procedures discussed in Sec. II, and final exclusion limits are presented at 95% confidence level. Regarding the limits from dark matter direct detection experiments, we show these bounds using the light-orange, light-cyan, and light-yellow region for the SBC-DM, XENON1T and PandaX-II experiments, respectively. Moreover, the light-red regions represent the exclusion limit of the relic density calculation for the given model, due to an overabundance of dark matter.

Bounds arising from the calculation of ΔN_{eff} by the BBN + CMB [71] measurements are shown using the vertical red band. It is to be noted that different electron beam dump experiments like E141 [74], E137 [73], E774 [75], KEK [76], Orsay [80], and NA64 [78], which put bounds on dark photon searches, can also put bounds on masses and couplings of Z' boson. Moreover, proton beam dump experiments like ν -CAL I [77], proton bremsstrahlung [82], CHARM [72], NOMAD [79], and PS191 [81] can also set bounds on Z' boson searches. We consider these bounds from the literature. In order to recast these limits, Darkcast [86] code has been utilized to our specific model, and the combined electron and proton beam dump limits are presented using light-green region at 90% confidence level.

We consider limits set by the proton-proton collider LHCb [84], where Z' arising from $U(1)'$ sym-

metry decays to $\mu^+\mu^-$. Similarly, we also consider Z' production in the electron-positron collider BABAR [83]. For both the LHCb and BABAR experiments, we have utilized Darkcast [86] code to recast their results as shown using the sky-blue and light-brown regions at 90% confidence level, respectively. Notice that for the BABAR, one could also have bound on $\mu^+\mu^-$ production [87], i.e., for scenarios where we have $x_e = 0, x_\mu \neq 0$. However, it has been observed that those bounds are much weaker compared to our COHERENT-CsI analysis or LHCb bounds [84]. Hence, throughout this work we only entertain bounds arising from the BABAR for $x_e \neq 0$.

We notice from the left panel of Fig. (2) that the forthcoming CE ν NS experiment SBC-CE ν NS will be able to produce the most stringent constraint for Z' masses between (0.02 – 1.3) GeV and couplings in the range ($10^{-5} - 4 \times 10^{-4}$). The reason for this is the high antineutrino flux (10^5 times higher than the one from the SNS) given the considered 1 MW_{th} power reactor and 3 m baseline [51, 52], the very low energy threshold achieved by the detector, and the fact that the background is greatly reduced due to the detector insensitivity to electron recoils, for more details see [44]. It can be observed that the SBC-CE ν NS will be able to constrain ($M_{Z'}, g'$) parameter space almost an $\mathcal{O}(1)$ stronger than the latest constraint provided by the COHERENT-CsI data. For the mass range between (0.2 – 1.3) GeV the future SBC-CE ν NS bounds will be competitive with the current LHCb exclusion limits. However, constraint coming from the BABAR collaboration puts the most stringent bounds in the range (0.5 – 10) GeV of $M'_{Z'}$, whereas above 10 GeV the LHCb again shows the best exclusion limits. Interestingly, for coupling of Z' boson $\sim 10^{-4}$ or smaller are concerned, it can be seen that the BBN+CMB calculations as well as beam dump bounds are able to rule out a significant amount of the parameter space for $M'_{Z'}$ less than 0.1 GeV (see shaded green and red regions). On the other hand, for $M'_{Z'}$ greater than 0.1 GeV, it is the relic density calculations that can rule out most of the parameter space for smaller g' as shown by the light-red regions.

We observe further that the forthcoming SBC-DM dark matter constraint will surpass the present bounds provided by XENON1T and PandaX-II, respectively. It is to be noted further that in this scenario, the right-handed neutrino mass matrix is generated dynamically, once the the scalar field ϕ_2 takes it's vev by breaking of $U(1)_{B-L}$ symmetry.

For the same model we also show the corresponding plot in the ($M_\chi - \sigma_{SI}$) plane in the right panel of Fig. (2), showing the same experimental constraints. The CE ν NS process from solar, atmospheric and diffuse supernova neutrinos constitute an unavoidable background for dark matter direct detection searches. We have indicated this background [85] with a dotted magenta curve in the results, as a discovery limit, not an exclusion region. We notice that the bounds from

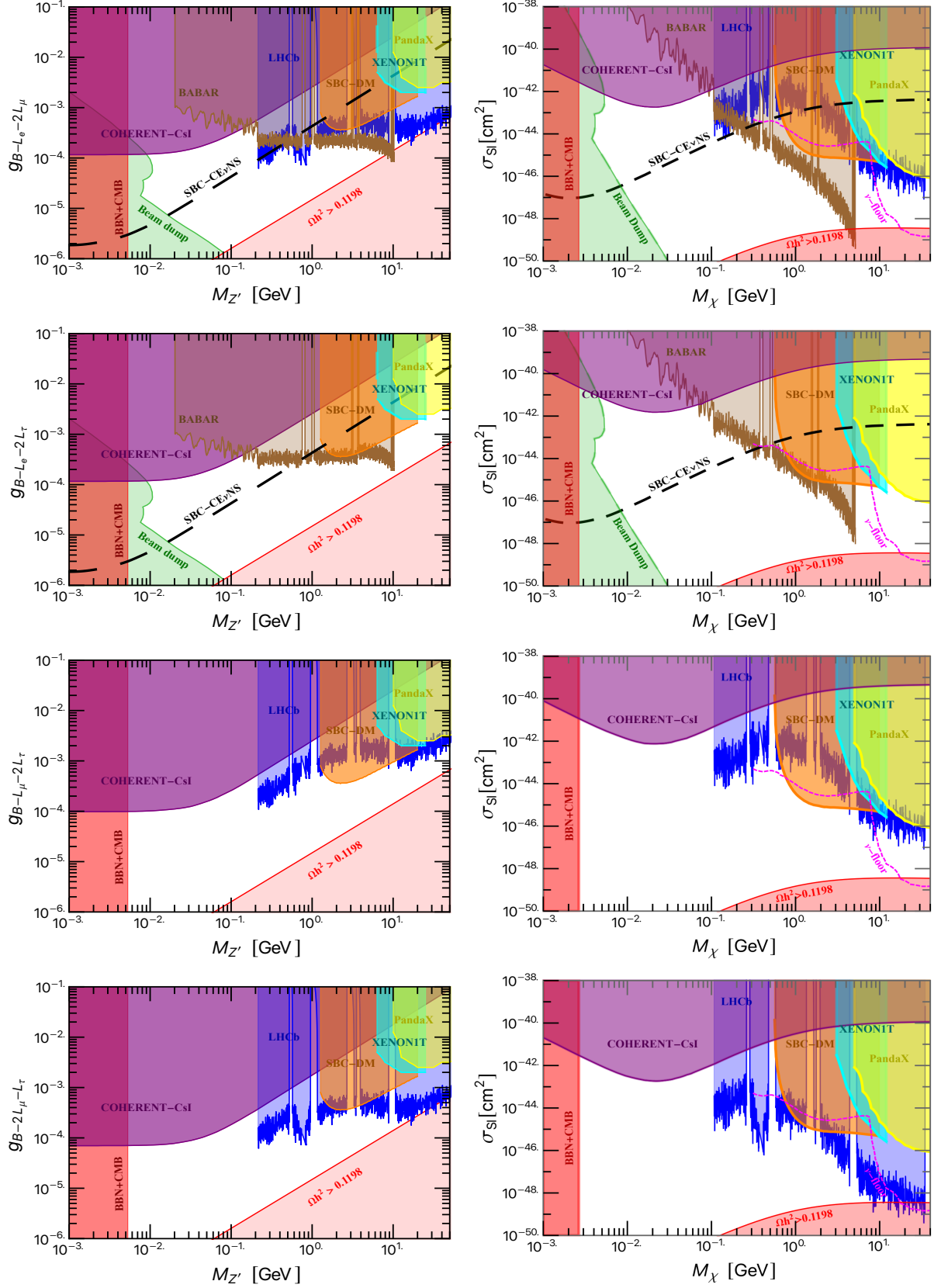


FIG. 3. Same as Fig. (2) but for MII $U(1)'$ models as given by Table (II).

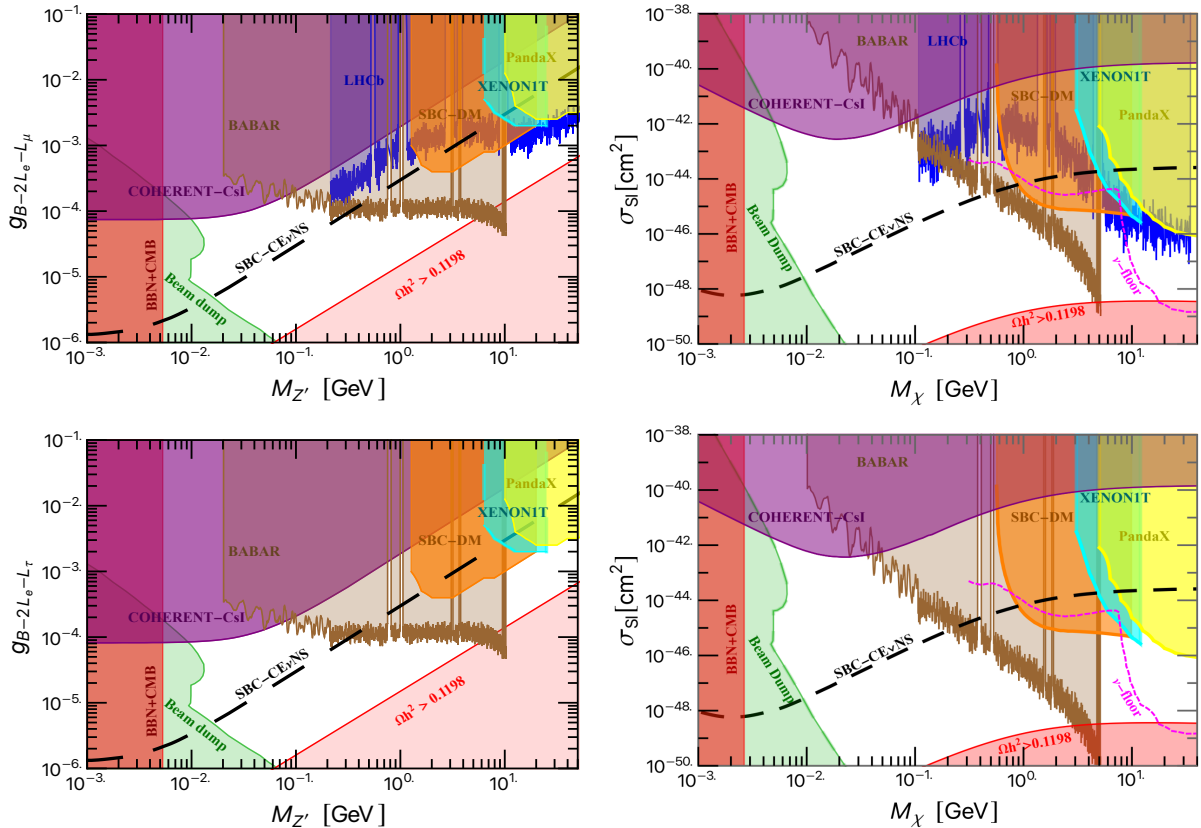


FIG. 4. Same as Fig. (2) but for the **MIII** $U(1)'$ models as given by Table (II).

BABAR and LHCb constrain the parameter space down to the neutrino floor of direct detection experiments, for dark matter masses below $M_\chi \sim 8$ GeV.

Having discussed the flavor-independent B-L model, we now proceed to explore parameter space for the flavor-dependent B-L models, which are presented in Fig. (3). The four scenarios investigated here correspond to the model **MII** as given by Table (II) and depending on $U(1)'$ charges (see Table (I)), we have $U(1)_{B-L_e-2L_\mu}$, $U(1)_{B-L_e-2L_\tau}$, $U(1)_{B-L_\mu-2L_\tau}$, and $U(1)_{B-2L_\mu-L_\tau}$, respectively. It is important to point out here that these four scenarios have very sharp predictions for the leptonic sector. All these cases lead to two-zero textures in the neutrino mass matrix, and are consistent with the latest global-fit of neutrino oscillation data, detailed phenomenology of these cases for the leptonic sector have been carried-out in [23].

Notice that beam dump experiments, BABAR as well as reactor experiment SBC-CE ν NS only provide bounds for the electron channel, therefore we find their impact only for the cases where one has non-zero x_e as can be seen from the first and second row of the Fig. (3). Similarly, the LHCb dark-photon searches are relevant for non-zero x_μ , and hence one sees its presence for three cases except for the second row (see sky-blue areas). In what follows, investigating all these four panels

it can be noticed that the first panel of the upper row shows the most stringently constrained region compared to the remaining cases. For all the possible charges, the constraints from direct DM searches translate into bounds for the $M_{Z'} - g'$ and we can also translate the different bounds from neutrino and accelerator experiments to the DM direct searches plane. For cases where we have non-zero x_e , there are constraints from beam dump, BABAR, COHERENT, and reactor neutrinos such as SBC-CE ν NS . While for non-zero x_μ there are bounds from COHERENT and LHCb experiments. Therefore, the most restricted allowed parameter space has been observed for these cases (i.e. for $x_e \neq 0 \neq x_\mu$). From the third and fourth row, we find that as there are no constraints from beam dump experiments or SBC-CE ν NS , most of the parameter space will remain unexplored. The unexplored regions for Z' boson masses lie in (5.3 – 60) MeV with the coupling constant below 10^{-4} as shown in the left panel. For DM masses, most of the unconstrained regions lie in (2.8 – 130) MeV (see right panel).

In Fig. (4), we discuss our numerical results for $U(1)'$ models corresponding to the model **MIII** as given by Table (II). All scenarios of models **MIII** have correlations for the neutrino masses and mixing parameters, see appendix A, and are compatible with the latest neutrino data.

As per the constrained parameter space is concerned, Fig. (4) shows almost similar pattern like Fig. (3). Here, we notice that the first row shows mildly better constraint compared to second row because of the presence of LHCb for the mass range above 10 GeV.

Our simulated results for models $U(1)_{B-3L_e}$, $U(1)_{B-3L_\mu}$, and $U(1)_{B-3L_\tau}$, are presented in Fig. (5), in the first, second and third rows respectively. Also, all cases of models **MIV** contains enough freedom to reproduce neutrino masses and mixing which are in good agreement with the latest neutrino data, but predict no correlations. Here again one observes that the first row shows the most restricted parameter space.

From the left panel of the second row it can be seen that the most of the parameter space in the range (5.3–60) MeV for g' below 10^{-4} remains unexplored. On the other hand, the left panel of the third row does not show any constraint in $(5.3 \times 10^{-3} - 0.1)$ GeV mass range of Z' , whereas above 0.1 GeV for coupling constant below 10^{-3} , the relic density calculation explored all the parameter space. Also, above 10 GeV of $M'_{Z'}$ mass with g' greater than 3×10^{-4} , it is the forthcoming SBC dark matter searches that can able to put the most strong bounds on the allowed parameter space. A similar conclusion holds true for the right panel, but for the DM mass in (2.8 – 130) MeV.

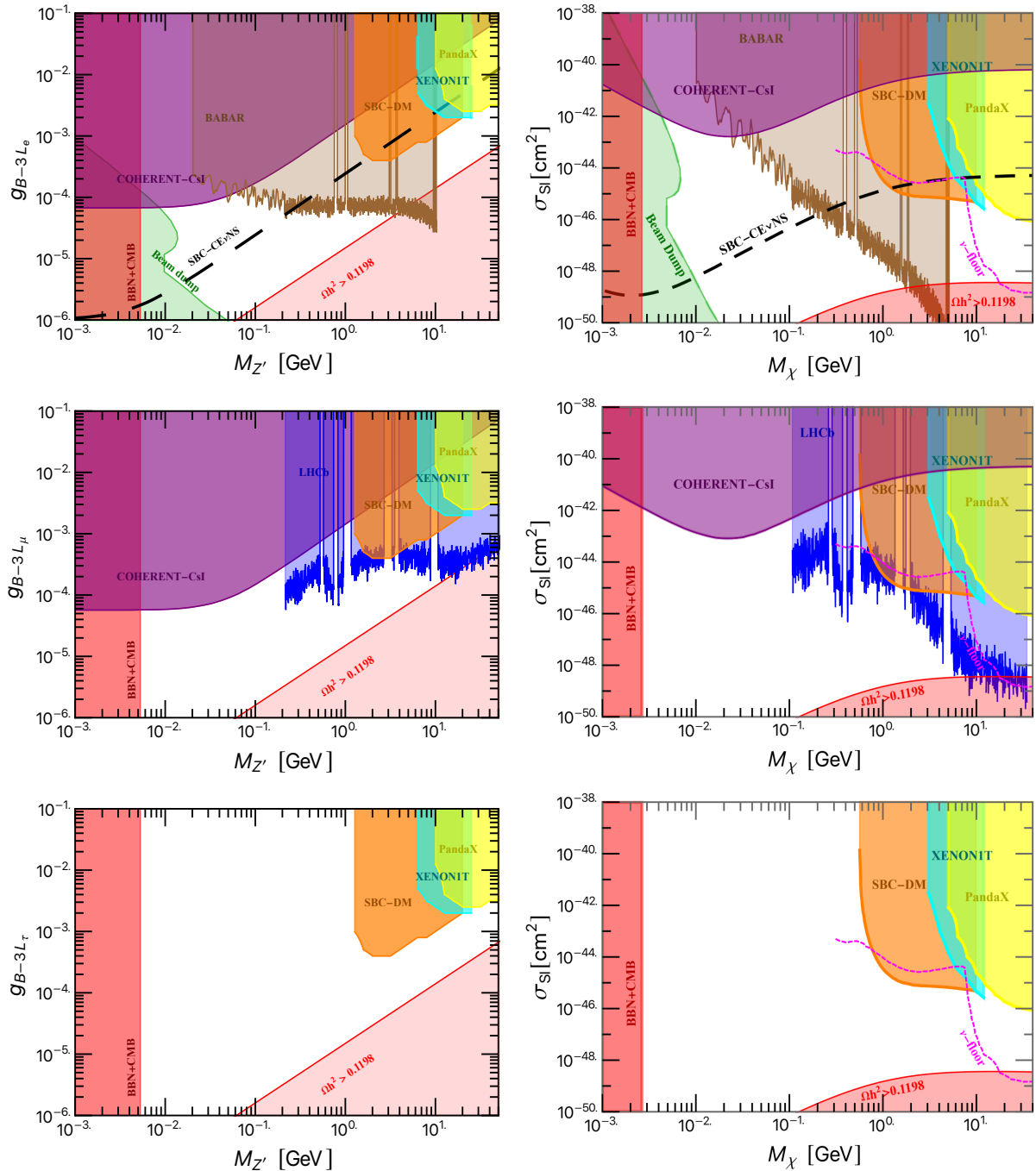


FIG. 5. Same as Fig. (2) but for MIV $U(1)'$ models as given by Table (III).

VI. CONCLUSIONS

We have discussed scenarios for a light gauge boson Z' , where the SM fermions and the DM interact with such a gauge boson. In these scenarios, the DM stability is due to a residual symmetry from the spontaneous breaking of $U(1)' \rightarrow Z_N$. We have found that in order to have the correct

thermal DM relic density, the DM annihilation in the early Universe must occur resonantly, i.e. DM mass should satisfy $M_\chi \approx M_{Z'}/2$. Firstly, the flavor-independent $U(1)'$ model i.e., $B - L$ scenario has been studied, where all leptons have the same charge. Later, different flavorful scenarios have also been analyzed, where different lepton flavors carry different $U(1)'$ charges. Since the quarks also transform under the extra gauge symmetry, the Z' couples to the nucleons, and therefore, we have investigated constraints arising from CE ν NS (when the electron and/or muon flavors are charged) as well as from DM direct detection experiments. However, it goes without saying that any new physics scenario beyond the SM undergoes various phenomenological constraints coming from numerous particle physics experiments. Using various other limits, coming from the beam dump, LHCb, and BABAR, we have first constrained $M_{Z'} - g'$ allowed parameter regions. Later, we have translated all these limits in the $M_\chi - \sigma_{\text{SI}}$ plane using the correlation between the DM mass (M_χ), spin-independent DM direct detection cross-section (σ_{SI}) together with gauge coupling (g').

Our noteworthy results are summarized in Figs. (2, 3, 4, and 5). Investigating all scenarios, it has been observed that the most stringent parameter space is obtained for the $U(1)'$ model with $x_e \neq 0$. For the particular scenario, we have bounds from the CE ν NS, beam dump, and BABAR together with DM direct detection experiments. As an example, from the first panel of Fig. (5) it can be noticed that the forthcoming reactor-based CE ν NS experiment SBC-CE ν NS can explore parameter space with gauge coupling of $\mathcal{O}(10^{-5})$ or smaller for Z' masses around 0.1 GeV. Also, we have observed that the future SBC-CE ν NS can put almost an order of magnitude stronger constraint compared to the latest COHERENT-CsI bound. On the other hand, the most unexplored regions are seen for scenarios with $x_e = 0, x_\mu = 0$, as there are no bounds from the CE ν NS, beam dump, LHCb, or BABAR. In this case, in the Z' mass range ($5.3 \times 10^{-3} - 0.1$) GeV parameter space remains unconstrained. From the DM relic density, there is a lower bound in the $M_{Z'} - g'$ plane due to kinematics. All these constraints can be translated to the DM direct detection cross-section setting strong constraints for DM masses below 10 GeV for PandaX-II, 6 GeV for XENON1T, whereas the stringent constraint is observed for the SBC-DM searches, which puts a limit around 1.3 GeV. Finally, it is worth mentioning that for DM mass below 1.3 GeV there are no constraints from the current experiments, and in this way, there is a complementarity in bounds from CE ν NS and DM direct searches.

ACKNOWLEDGMENTS

This work is supported by the German-Mexican research collaboration grant SP 778/4-1 (DFG) and 278017 (CONACYT), the grants CONACYT CB-2017-2018/A1-S-13051 (México), the DGAPA UNAM grant PAPIIT IN107621 and SNI (México). NN is supported by the postdoctoral fellowship program DGAPA-UNAM. LMGDLV is supported by CONACYT. The work of LJF is supported by a CONACYT postdoctoral fellowship.

Appendix A: Correlations in the MIII models

In the models $B - 2L_e - L_\mu$ and $B - 2L_e - L_\tau$, the charged lepton and Dirac neutrino mass matrices are diagonal by construction. While it is not enough to include the ϕ_1 and ϕ_2 to reproduce neutrino masses and mixings [23]. This can be alleviated by the inclusion of a third flavon field ϕ_4 . In this way the right-handed neutrino mass matrix takes the form

$$M_{B-2L_e-L_\mu} = \begin{pmatrix} y_4 v_4 & 0 & y_2 v_2 \\ 0 & y_3 v_2 & y_1 v_1 \\ y_2 v_2 & y_1 v_1 & M_1 \end{pmatrix}, M_{B-2L_e-L_\tau} = \begin{pmatrix} y_4 v_4 & y_2 v_2 & 0 \\ y_2 v_2 & M_1 & y_1 v_1 \\ 0 & y_1 v_1 & y_3 v_2 \end{pmatrix}, \quad (\text{A1})$$

for $U'_{B-2L_e-L_\mu}$, $U'_{B-2L_e-L_\tau}$ models, respectively. Given the Dirac and Majorana neutrino mass matrices, one can construct the low-energy active neutrino mass matrices using type-I seesaw mechanism. We write the active neutrino mass matrix as

$$m_\nu = \begin{pmatrix} m_{11} & m_{12} & m_{13} \\ * & m_{22} & m_{23} \\ * & * & m_{33} \end{pmatrix}. \quad (\text{A2})$$

From the parameters in Eq. (A1), we find following correlations

$$\begin{aligned} m_{12}m_{33} &= m_{13}m_{23}, \\ m_{12}m_{23} &= m_{13}m_{22}, \end{aligned} \quad (\text{A3})$$

for $U(1)_{B-2L_e-L_\mu}$ and $U(1)_{B-2L_e-L_\tau}$, respectively. We have found that these correlations are compatible with current oscillation data, with the correct choice of neutrino masses and Majorana phases. For the MIV models there are no correlations in the mass matrix, there is enough freedom

to fit neutrino oscillation data.

-
- [1] **COHERENT** Collaboration, D. Akimov et al., *Observation of Coherent Elastic Neutrino-Nucleus Scattering*, *Science* **357** (2017), no. 6356 1123–1126, [[arXiv:1708.01294](#)].
- [2] D. Z. Freedman, *Coherent Neutrino Nucleus Scattering as a Probe of the Weak Neutral Current*, *Phys. Rev. D* **9** (1974) 1389–1392.
- [3] **COHERENT** Collaboration, D. Akimov et al., *First Measurement of Coherent Elastic Neutrino-Nucleus Scattering on Argon*, *Phys. Rev. Lett.* **126** (2021), no. 1 012002, [[arXiv:2003.10630](#)].
- [4] **COHERENT** Collaboration, D. Akimov et al., *COHERENT Collaboration data release from the first detection of coherent elastic neutrino-nucleus scattering on argon*, [arXiv:2006.12659](#).
- [5] K. Scholberg, *Prospects for measuring coherent neutrino-nucleus elastic scattering at a stopped-pion neutrino source*, *Phys. Rev. D* **73** (2006) 033005, [[hep-ex/0511042](#)].
- [6] M. Lindner, W. Rodejohann, and X.-J. Xu, *Coherent Neutrino-Nucleus Scattering and new Neutrino Interactions*, *JHEP* **03** (2017) 097, [[arXiv:1612.04150](#)].
- [7] B. Sevda et al., *Constraints on nonstandard intermediate boson exchange models from neutrino-electron scattering*, *Phys. Rev. D* **96** (2017), no. 3 035017, [[arXiv:1702.02353](#)].
- [8] O. G. Miranda, D. K. Papoulias, M. Tórtola, and J. W. F. Valle, *Probing neutrino transition magnetic moments with coherent elastic neutrino-nucleus scattering*, *JHEP* **07** (2019) 103, [[arXiv:1905.03750](#)].
- [9] M. Cadeddu, C. Giunti, Y. F. Li, and Y. Y. Zhang, *Average CsI neutron density distribution from COHERENT data*, *Phys. Rev. Lett.* **120** (2018), no. 7 072501, [[arXiv:1710.02730](#)].
- [10] D. K. Papoulias, T. S. Kosmas, R. Sahu, V. K. B. Kota, and M. Hota, *Constraining nuclear physics parameters with current and future COHERENT data*, *Phys. Lett. B* **800** (2020) 135133, [[arXiv:1903.03722](#)].
- [11] B. C. Canas, E. A. Garcés, O. G. Miranda, A. Parada, and G. Sanchez Garcia, *Interplay between nonstandard and nuclear constraints in coherent elastic neutrino-nucleus scattering experiments*, *Phys. Rev. D* **101** (2020), no. 3 035012, [[arXiv:1911.09831](#)].
- [12] M. Cadeddu, F. Dordei, C. Giunti, Y. F. Li, E. Picciau, and Y. Y. Zhang, *Physics results from the first COHERENT observation of coherent elastic neutrino-nucleus scattering in argon and their combination with cesium-iodide data*, *Phys. Rev. D* **102** (2020), no. 1 015030, [[arXiv:2005.01645](#)].
- [13] M. Cadeddu, C. Giunti, K. A. Kouzakov, Y. F. Li, A. I. Studenikin, and Y. Y. Zhang, *Neutrino Charge Radii from COHERENT Elastic Neutrino-Nucleus Scattering*, *Phys. Rev. D* **98** (2018), no. 11 113010, [[arXiv:1810.05606](#)]. [Erratum: *Phys.Rev.D* 101, 059902 (2020)].
- [14] O. G. Miranda, G. Sanchez Garcia, and O. Sanders, *Coherent elastic neutrino-nucleus scattering as a precision test for the Standard Model and beyond: the COHERENT proposal case*, *Adv. High Energy*

- Phys.* **2019** (2019) 3902819, [[arXiv:1902.09036](#)].
- [15] C. Blanco, D. Hooper, and P. Machado, *Constraining Sterile Neutrino Interpretations of the LSND and MiniBooNE Anomalies with Coherent Neutrino Scattering Experiments*, [arXiv:1901.08094](#).
- [16] J. M. Berryman, *Constraining Sterile Neutrino Cosmology with Terrestrial Oscillation Experiments*, *Phys. Rev.* **D100** (2019), no. 2 023540, [[arXiv:1905.03254](#)].
- [17] O. G. Miranda, D. K. Papoulias, O. Sanders, M. Tórtola, and J. W. F. Valle, *Future CEvNS experiments as probes of lepton unitarity and light-sterile neutrinos*, *Phys. Rev. D* **102** (2020) 113014, [[arXiv:2008.02759](#)].
- [18] J. Liao and D. Marfatia, *COHERENT constraints on nonstandard neutrino interactions*, *Phys. Lett.* **B775** (2017) 54–57, [[arXiv:1708.04255](#)].
- [19] C. Giunti, *General COHERENT Constraints on Neutrino Non-Standard Interactions*, [arXiv:1909.00466](#).
- [20] I. Esteban, M. C. Gonzalez-Garcia, and M. Maltoni, *On the Determination of Leptonic CP Violation and Neutrino Mass Ordering in Presence of Non-Standard Interactions: Present Status*, *JHEP* **06** (2019) 055, [[arXiv:1905.05203](#)].
- [21] P. Coloma, I. Esteban, M. C. Gonzalez-Garcia, and M. Maltoni, *Improved global fit to Non-Standard neutrino Interactions using COHERENT energy and timing data*, *JHEP* **02** (2020) 023, [[arXiv:1911.09109](#)].
- [22] A. N. Khan and W. Rodejohann, *New physics from COHERENT data with an improved quenching factor*, *Phys. Rev.* **D100** (2019), no. 11 113003, [[arXiv:1907.12444](#)].
- [23] L. J. Flores, N. Nath, and E. Peinado, *Non-standard neutrino interactions in $U(1)'$ model after COHERENT data*, *JHEP* **06** (2020) 045, [[arXiv:2002.12342](#)].
- [24] P. Coloma, M. C. Gonzalez-Garcia, and M. Maltoni, *Neutrino oscillation constraints on $U(1)'$ models: from non-standard interactions to long-range forces*, *JHEP* **01** (2021) 114, [[arXiv:2009.14220](#)].
- [25] **XENON** Collaboration, E. Aprile et al., *Search for Coherent Elastic Scattering of Solar 8B Neutrinos in the XENON1T Dark Matter Experiment*, *Phys. Rev. Lett.* **126** (2021) 091301, [[arXiv:2012.02846](#)].
- [26] **PandaX-II** Collaboration, X. Cui et al., *Dark Matter Results From 54-Ton-Day Exposure of PandaX-II Experiment*, *Phys. Rev. Lett.* **119** (2017), no. 18 181302, [[arXiv:1708.06917](#)].
- [27] J.-H. Huh, J. E. Kim, J.-C. Park, and S. C. Park, *Galactic 511 keV line from MeV milli-charged dark matter*, *Phys. Rev. D* **77** (2008) 123503, [[arXiv:0711.3528](#)].
- [28] M. Pospelov, A. Ritz, and M. B. Voloshin, *Secluded WIMP Dark Matter*, *Phys. Lett. B* **662** (2008) 53–61, [[arXiv:0711.4866](#)].
- [29] D. Hooper and K. M. Zurek, *A Natural Supersymmetric Model with MeV Dark Matter*, *Phys. Rev. D* **77** (2008) 087302, [[arXiv:0801.3686](#)].
- [30] C. Cheung, J. T. Ruderman, L.-T. Wang, and I. Yavin, *Kinetic Mixing as the Origin of Light Dark Scales*, *Phys. Rev. D* **80** (2009) 035008, [[arXiv:0902.3246](#)].

- [31] R. Essig, J. Kaplan, P. Schuster, and N. Toro, *On the Origin of Light Dark Matter Species*, [arXiv:1004.0691](#).
- [32] R. Essig et al., *Working Group Report: New Light Weakly Coupled Particles*, in *Community Summer Study 2013: Snowmass on the Mississippi*, 10, 2013. [arXiv:1311.0029](#).
- [33] B. Batell, P. deNiverville, D. McKeen, M. Pospelov, and A. Ritz, *Leptophobic Dark Matter at Neutrino Factories*, *Phys. Rev. D* **90** (2014), no. 11 115014, [[arXiv:1405.7049](#)].
- [34] **COHERENT** Collaboration, D. Akimov et al., *Sensitivity of the COHERENT Experiment to Accelerator-Produced Dark Matter*, *Phys. Rev. D* **102** (2020), no. 5 052007, [[arXiv:1911.06422](#)].
- [35] M. Cvetič and P. Langacker, *Z' Physics and Supersymmetry*, *Adv. Ser. Direct. High Energy Phys.* **18** (1998) 312–331, [[hep-ph/9707451](#)].
- [36] E. J. Chun and J.-C. Park, *Dark matter and sub-GeV hidden U(1) in GMSB models*, *JCAP* **02** (2009) 026, [[arXiv:0812.0308](#)].
- [37] M. Frank, *Evading Z' boson mass limits in U(1)' supersymmetric models*, *Eur. Phys. J. ST* **229** (2020), no. 21 3205–3220.
- [38] D. London and J. L. Rosner, *Extra Gauge Bosons in E(6)*, *Phys. Rev. D* **34** (1986) 1530.
- [39] J. L. Hewett and T. G. Rizzo, *Low-Energy Phenomenology of Superstring Inspired E(6) Models*, *Phys. Rept.* **183** (1989) 193.
- [40] G. Arcadi, M. Lindner, Y. Mambrini, M. Pierre, and F. S. Queiroz, *GUT Models at Current and Future Hadron Colliders and Implications to Dark Matter Searches*, *Phys. Lett. B* **771** (2017) 508–514, [[arXiv:1704.02328](#)].
- [41] M. Cvetič and P. Langacker, *Implications of Abelian extended gauge structures from string models*, *Phys. Rev. D* **54** (1996) 3570–3579, [[hep-ph/9511378](#)].
- [42] G. Cleaver, M. Cvetič, J. R. Espinosa, L. L. Everett, P. Langacker, and J. Wang, *Physics implications of flat directions in free fermionic superstring models 1. Mass spectrum and couplings*, *Phys. Rev. D* **59** (1999) 055005, [[hep-ph/9807479](#)].
- [43] **SBC** Collaboration, P. Giampa, *The Scintillating Bubble Chamber (SBC) Experiment for Dark Matter and Reactor CEvNS*, *PoS ICHEP2020* (2021) 632.
- [44] **SBC, CEvNS Theory Group at IF-UNAM** Collaboration, L. J. Flores et al., *Physics reach of a low threshold scintillating argon bubble chamber in coherent elastic neutrino-nucleus scattering reactor experiments*, *Phys. Rev. D* **103** (2021), no. 9 L091301, [[arXiv:2101.08785](#)].
- [45] **COHERENT** Collaboration, D. Akimov et al., *First Measurement of Coherent Elastic Neutrino-Nucleus Scattering on Argon*, *Phys. Rev. Lett.* **126** (2021), no. 1 012002, [[arXiv:2003.10630](#)].
- [46] A. Drukier and L. Stodolsky, *Principles and Applications of a Neutral Current Detector for Neutrino Physics and Astronomy*, *Phys. Rev. D* **30** (1984) 2295.
- [47] J. Barranco, O. G. Miranda, and T. I. Rashba, *Probing new physics with coherent neutrino scattering off nuclei*, *JHEP* **12** (2005) 021, [[hep-ph/0508299](#)].

- [48] K. Patton, J. Engel, G. C. McLaughlin, and N. Schunck, *Neutrino-nucleus coherent scattering as a probe of neutron density distributions*, *Phys. Rev.* **C86** (2012) 024612, [[arXiv:1207.0693](#)].
- [49] O. G. Miranda, D. K. Papoulias, G. Sanchez Garcia, O. Sanders, M. Tórtola, and J. W. F. Valle, *Implications of the first detection of coherent elastic neutrino-nucleus scattering (CEvNS) with Liquid Argon*, *JHEP* **05** (2020) 130, [[arXiv:2003.12050](#)]. [Erratum: *JHEP* 01, 067 (2021)].
- [50] M. Cadeddu, N. Cargioli, F. Dordei, C. Giunti, Y. F. Li, E. Picciau, and Y. Y. Zhang, *Constraints on light vector mediators through coherent elastic neutrino nucleus scattering data from COHERENT*, *JHEP* **01** (2021) 116, [[arXiv:2008.05022](#)].
- [51] P. Huber, *On the determination of anti-neutrino spectra from nuclear reactors*, *Phys. Rev. C* **84** (2011) 024617, [[arXiv:1106.0687](#)]. [Erratum: *Phys.Rev.C* 85, 029901 (2012)].
- [52] T. Mueller et al., *Improved Predictions of Reactor Antineutrino Spectra*, *Phys. Rev. C* **83** (2011) 054615, [[arXiv:1101.2663](#)].
- [53] J. Heeck, M. Lindner, W. Rodejohann, and S. Vogl, *Non-Standard Neutrino Interactions and Neutral Gauge Bosons*, *SciPost Phys.* **6** (2019), no. 3 038, [[arXiv:1812.04067](#)].
- [54] T. Han, J. Liao, H. Liu, and D. Marfatia, *Nonstandard neutrino interactions at COHERENT, DUNE, T2HK and LHC*, *JHEP* **11** (2019) 028, [[arXiv:1910.03272](#)].
- [55] M. Bauer, P. Foldenauer, and M. Mosny, *Flavor structure of anomaly-free hidden photon models*, *Phys. Rev. D* **103** (2021), no. 7 075024, [[arXiv:2011.12973](#)].
- [56] L. M. Krauss and F. Wilczek, *Discrete Gauge Symmetry in Continuum Theories*, *Phys. Rev. Lett.* **62** (1989) 1221.
- [57] C. Bonilla, S. Centelles-Chuliá, R. Cepedello, E. Peinado, and R. Srivastava, *Dark matter stability and Dirac neutrinos using only Standard Model symmetries*, *Phys. Rev. D* **101** (2020), no. 3 033011, [[arXiv:1812.01599](#)].
- [58] C. Bonilla, E. Peinado, and R. Srivastava, *The role of residual symmetries in dark matter stability and the neutrino nature*, *LHEP* **2** (2019), no. 1 124, [[arXiv:1903.01477](#)].
- [59] N. Okada and S. Okada, *Z'_{BL} portal dark matter and LHC Run-2 results*, *Phys. Rev. D* **93** (2016), no. 7 075003, [[arXiv:1601.07526](#)].
- [60] M. Escudero, S. J. Witte, and N. Rius, *The dispirited case of gauged $U(1)_{B-L}$ dark matter*, *JHEP* **08** (2018) 190, [[arXiv:1806.02823](#)].
- [61] S. Okada, *Z' Portal Dark Matter in the Minimal $B - L$ Model*, *Adv. High Energy Phys.* **2018** (2018) 5340935, [[arXiv:1803.06793](#)].
- [62] C. Han, M. L. López-Ibáñez, B. Peng, and J. M. Yang, *Dirac dark matter in $U(1)_{B-L}$ with the Stueckelberg mechanism*, *Nucl. Phys. B* **959** (2020) 115154, [[arXiv:2001.04078](#)].
- [63] D. Borah, S. Jyoti Das, and A. K. Saha, *Cosmic inflation in minimal $U(1)_{B-L}$ model: implications for (non) thermal dark matter and leptogenesis*, *Eur. Phys. J. C* **81** (2021), no. 2 169, [[arXiv:2005.11328](#)].

- [64] K. Kaneta, Z. Kang, and H.-S. Lee, *Right-handed neutrino dark matter under the $B - L$ gauge interaction*, *JHEP* **02** (2017) 031, [[arXiv:1606.09317](#)].
- [65] A. Alves, G. Arcadi, Y. Mambrini, S. Profumo, and F. S. Queiroz, *Augury of darkness: the low-mass dark Z' portal*, *JHEP* **04** (2017) 164, [[arXiv:1612.07282](#)].
- [66] D. Borah, D. Nanda, N. Narendra, and N. Sahu, *Right-handed neutrino dark matter with radiative neutrino mass in gauged $B - L$ model*, *Nucl. Phys. B* **950** (2020) 114841, [[arXiv:1810.12920](#)].
- [67] A. Semenov, *LanHEP: A Package for the automatic generation of Feynman rules in field theory. Version 3.0*, *Comput. Phys. Commun.* **180** (2009) 431–454, [[arXiv:0805.0555](#)].
- [68] G. Bélanger, F. Boudjema, A. Goudelis, A. Pukhov, and B. Zaldivar, *micrOMEGAs5.0 : Freeze-in*, *Comput. Phys. Commun.* **231** (2018) 173–186, [[arXiv:1801.03509](#)].
- [69] **Planck** Collaboration, N. Aghanim et al., *Planck 2018 results. VI. Cosmological parameters*, *Astron. Astrophys.* **641** (2020) A6, [[arXiv:1807.06209](#)].
- [70] A. Alves, A. Berlin, S. Profumo, and F. S. Queiroz, *Dark Matter Complementarity and the Z' Portal*, *Phys. Rev. D* **92** (2015), no. 8 083004, [[arXiv:1501.03490](#)].
- [71] A. Kamada and H.-B. Yu, *Coherent Propagation of PeV Neutrinos and the Dip in the Neutrino Spectrum at IceCube*, *Phys. Rev.* **D92** (2015), no. 11 113004, [[arXiv:1504.00711](#)].
- [72] **CHARM** Collaboration, F. Bergsma et al., *Search for Axion Like Particle Production in 400-GeV Proton - Copper Interactions*, *Phys. Lett.* **157B** (1985) 458–462.
- [73] J. D. Bjorken, S. Ecklund, W. R. Nelson, A. Abashian, C. Church, B. Lu, L. W. Mo, T. A. Nunamaker, and P. Rassmann, *Search for neutral metastable penetrating particles produced in the SLAC beam dump*, *Phys. Rev.* **D38** (1988) 3375.
- [74] E. M. Riordan et al., *Search for short-lived axions in an electron-beam-dump experiment*, *Phys. Rev. Lett.* **59** (1987) 755.
- [75] A. Bross, M. Crisler, S. H. Pordes, J. Volk, S. Errede, and J. Wrbanek, *A search for short-lived particles produced in an electron beam dump*, *Phys. Rev. Lett.* **67** (1991) 2942–2945.
- [76] A. Konaka et al., *Search for neutral particles in electron-beam-dump experiment*, *Phys. Rev. Lett.* **57** (1986) 659.
- [77] J. Blümlein et al., *Limits on neutral light scalar and pseudoscalar particles in a proton beam dump experiment*, *Z. Phys.* **C51** (1991) 341–350.
- [78] **NA64** Collaboration, D. Banerjee et al., *Improved limits on a hypothetical $X(16.7)$ boson and a dark photon decaying into e^+e^- pairs*, [arXiv:1912.11389](#).
- [79] **NOMAD** Collaboration, P. Astier et al., *Search for heavy neutrinos mixing with tau neutrinos*, *Phys. Lett.* **B506** (2001) 27–38, [[hep-ex/0101041](#)].
- [80] M. Davier and H. Nguyen Ngoc, *An Unambiguous Search for a Light Higgs Boson*, *Phys. Lett.* **B229** (1989) 150–155.
- [81] G. Bernardi et al., *Search for neutrino decay*, *Phys. Lett.* **B166** (1986) 479.

- [82] J. Blümlein and J. Brunner, *New exclusion limits on dark gauge forces from proton bremsstrahlung in beam-dump data*, *Phys. Lett.* **B731** (2014) 320–326, [[arXiv:1311.3870](#)].
- [83] **BaBar** Collaboration, J. P. Lees et al., *Search for a dark photon in e^+e^- collisions at BaBar*, *Phys. Rev. Lett.* **113** (2014) 201801, [[arXiv:1406.2980](#)].
- [84] **LHCb** Collaboration, R. Aaij et al., *Search for $A' \rightarrow \mu^+\mu^-$ decays*, *Phys. Rev. Lett.* **124** (2020), no. 4 041801, [[arXiv:1910.06926](#)].
- [85] F. Ruppin, J. Billard, E. Figueroa-Feliciano, and L. Strigari, *Complementarity of dark matter detectors in light of the neutrino background*, *Phys. Rev. D* **90** (2014), no. 8 083510, [[arXiv:1408.3581](#)].
- [86] P. Ilten, Y. Soreq, M. Williams, and W. Xue, *Serendipity in dark photon searches*, *JHEP* **06** (2018) 004, [[arXiv:1801.04847](#)].
- [87] **BaBar** Collaboration, J. P. Lees et al., *Search for a muonic dark force at BABAR*, *Phys. Rev. D* **94** (2016), no. 1 011102, [[arXiv:1606.03501](#)].